

# Experimental Investigation into Flue Gas Water and Waste Heat Recovery Using a Purge Gas Ceramic Membrane Condenser

Da Teng, Xinxian Jia, Wenkai Yang, Liansuo An, Guoqing Shen,\* and Heng Zhang



Cite This: *ACS Omega* 2022, 7, 4956–4969



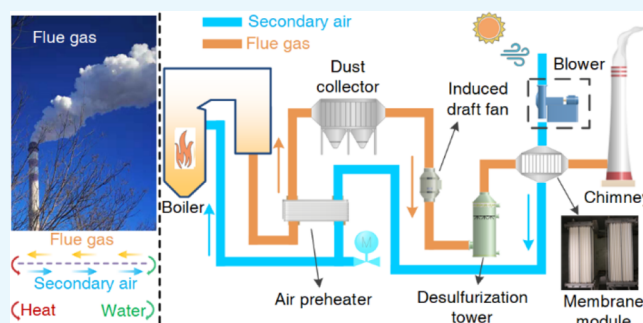
Read Online

ACCESS |

Metrics & More

Article Recommendations

**ABSTRACT:** The direct discharge of wet saturated flue gas from a coal-fired power plant boiler causes a lot of water and waste heat loss. An inorganic ceramic membrane condenser recovers water and waste heat from the flue gas, which has great significance to improve energy utilization efficiency and reduce water consumption. However, the flue gas temperature is relatively low; thus, it is difficult to effectively utilize waste heat. In this paper, it is attempted to use the boiler secondary air as the cooling medium of the ceramic membrane condenser to realize the flue gas waste heat reuse. Based on the above ideas, a purge gas ceramic membrane condenser experimental platform was built for the water and waste heat recovery from the flue gas, and the water and waste heat recovery characteristics and the purge gas outlet parameters were discussed. Simultaneously, the heat transfer resistance and water recovery power consumption are also analyzed. The experimental results show that the water and waste heat recovery characteristics are enhanced with the purge gas flow increases. Increasing the flue gas temperature will increase the water recovery rate and heat recovery power. The ceramic membrane transmission efficiency is a key factor in restricting the actual water recovery efficiency. The purge gas absorbs the water and waste heat from the flue gas, the purge gas temperature and moisture content are significantly increased, and the purge gas relative humidity is also close to saturation. The Biot number of the ceramic membrane condenser is about  $3.2 \times 10^{-3}$  to  $1.9 \times 10^{-2}$ ; thus, the ceramic membrane tube wall thermal resistance can be neglected. There is a temperature difference between the flue gas and the purge gas, and the entropy production value of the ceramic membrane condenser increases with the flue gas temperature increases by the irreversible process.



## 1. INTRODUCTION

Since the 21st century, China's economy has developed rapidly. The electricity supply as an important support has also grown significantly.<sup>1</sup> In 2019, the traditional coal-fired generation capacity is about  $4.9 \times 10^6$  GWh, accounting for 65% of the total power generation capacity in China. Therefore, it is still very important to carry out research on energy saving and consumption reduction of coal-fired power plants to achieve energy sustainable development.

Currently, the acidic substance content varies widely in coal combustion. In order to avoid low-temperature corrosion,<sup>2,3</sup> the exhaust temperature of a coal-fired power plant boiler is generally 110–150 °C. In China, the wet desulfurization process is commonly used in coal-fired power plants to remove acid gases from the flue gas, and the wet saturated flue gas temperature is about 50–60 °C at the desulfurization tower outlet. The direct discharge of the flue gas causes a large amount of waste heat loss, and a lot of water vapor is directly discharged to the atmosphere, which intensifies the energy consumption and water resource waste.<sup>4,5</sup> If water is effectively recovered from the flue gas, then water vapor latent heat is released and it will have a double positive effect on improving

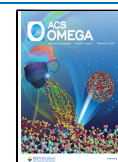
the energy utilization efficiency and reducing the power generation water consumption.<sup>6</sup> Moreover, reducing the flue gas moisture content helps dissipate pollutants, improves the environment around the power plant, and effectively reduces the “gypsum rain” phenomenon.

For a long time, many researchers have been concerned with the flue gas water and waste heat recovery technology research.<sup>7–9</sup> The low-temperature condensation method<sup>10–12</sup> uses a cooling medium to reduce the flue gas temperature, forcing the water vapor to condense and precipitate in the flue gas, thus achieving sensible heat recovery and latent heat recovery. The liquid absorption method<sup>13–15</sup> uses a dehumidification solution with low saturated water vapor pressure to absorb water vapor from the flue gas. The dehumidification

Received: October 8, 2021

Accepted: January 21, 2022

Published: February 1, 2022



solution temperature is slightly higher than the conventional cooling medium temperature, which helps to realize the extensive use of flue gas waste heat. Common dehumidification solutions include lithium bromide, lithium chloride, calcium chloride, etc. The membrane separation method<sup>16,17</sup> is driven by the pressure difference; the water vapor and other gases' permeation rates are different in the membrane material, relying on the high selectivity of the membrane material to achieve clean water recovery.

Based on the membrane separation method, the flue gas dehydration process can obtain higher-quality condensate water<sup>18</sup> and has a strong waste heat recovery capacity. Membrane materials are the key to the membrane separation method, which can be classified as hollow fiber membranes or porous ceramic membranes. With the support of the European Union, the CAPWA project uses hollow fiber membranes to recover water from the flue gas. A vacuum is maintained inside the membrane. The water vapor enters inside the membrane through a dissolution–diffusion process to achieve water recovery from the flue gas. Brunetti et al.<sup>19</sup> used hydrophobic PVDF hollow fiber membranes to form a membrane condenser. Due to the hydrophobic characteristics of membrane materials, the water vapor condensation phenomenon occurred on the flue gas side. Research shows that the water vapor partial pressure difference is the key factor affecting the water recovery efficiency. Chen et al.<sup>20</sup> studied the water recovery characteristics based on hydrophilic SPEEK/PES hollow fiber membranes and found that a higher degree of sulfonation corresponds to a larger selective separation coefficient. The key problem of hollow fiber membranes is the low water recovery flux.<sup>21,22</sup> Compared with organic hollow fiber membranes, inorganic porous ceramic membranes have the advantages of acid and alkali resistance, high temperature resistance, and high mechanical strength. The U.S. Department of Energy (DOE) has developed a transport membrane condenser technology. The flue gas flows inside the ceramic membrane, and the boiler feed water flows outside the ceramic membrane. The water vapor condensation passes through the porous ceramic membrane into the boiler feed water side. The membrane condenser technology enables the use of flue gas condensate water as boiler feed water. As shown in Table 1, the flue gas and cooling water parameters are important factors affecting the operating characteristics of the porous ceramic membrane condenser.<sup>23</sup> The ceramic membrane pore size is directly related to the water transport process. Compared with dense membranes, porous ceramic membranes can obtain a higher water recovery flux. Based on the Kelvin equation, there is capillary condensation in the hydrophilic ceramic membranes with a 2–50 nm pore size. Chen et al.<sup>24</sup> used 20 nm pore size ceramic membranes to achieve water recovery from the flue gas. When the cooling water temperature is higher than the flue gas dew point temperature, there is still a small water recovery flux.

There are also many research scholars who focus on the waste heat recovery characteristics for the membrane separation method. Compared with the low-temperature condensation method, the membrane separation method has a higher waste heat recovery flux.<sup>17,31</sup> Bao et al.<sup>32</sup> compared nanometer ceramic membrane tubes and stainless steel tubes with the same structural parameters and applied both to the flue gas waste heat recovery. The convection Nusselt number is 50–80% higher for nanometer ceramic membrane tubes. Wang<sup>33</sup> found that the capillary condensation phenomenon of

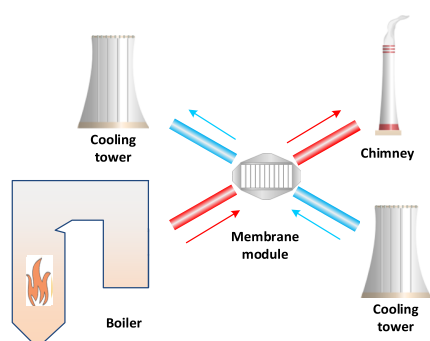
**Table 1. Operating Characteristics of the Ceramic Membrane Condenser<sup>a</sup>**

literature	factors	water recovery		heat recovery	
		flux	efficiency	flux	efficiency
refs 25, 26	flue gas temperature↑	↑	↑	↑	↑
refs 27, 28		↑	—	↑	—
refs 25, 29, 30	flue gas flow↑	↑	↓	↑	↓
ref 27		↑	—	↑	—
ref 26	relative humidity↑	↑	↑	↑	↓
ref 27		↑	—	↑	—
ref 26	cooling water flow↑	↑	↑	↑	↑
refs 29, 30		↑	↑	↑	↑
ref 25		→	→	→	→
refs 27, 28		↑	—	↑	—
refs 25, 29	cooling water temperature↑	↓	↓	↓	↓
refs 27, 28		↓	—	↓	—
ref 26		↓	—	—	—

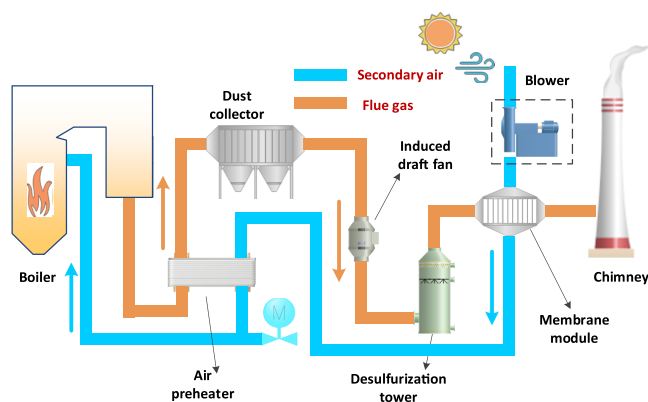
<sup>a</sup>↑: Increase. →: Basically unchanged. ↑: Increase first and then stabilize. ↓: Decrease. —: Not covered in the literature.

porous ceramic membranes helps to enhance heat transfer. The ceramic membrane penetration process can reduce the thermal resistance of the condensation water liquid film; thus, the Nusselt number of the ceramic membrane tube is higher than the Nusselt number of the stainless steel tube. Yue et al.<sup>34</sup> compared the multichannel ceramic membrane tube and the single-channel ceramic membrane tube heat transfer process. Both of them are mainly convective heat transfer, but the heat transfer resistance of the multichannel ceramic membrane tube is higher than the heat transfer resistance of the single-channel ceramic membrane tube. During the flue gas dehydration process, water vapor releases latent heat, which causes the flue gas waste heat recovery to be dominated by latent heat recovery.<sup>27,28,35</sup>

The research team also did a lot of research work in the early stage,<sup>17,20,22,24,26,28,29,36–38</sup> and carried out a pilot test for the water and waste heat recovery from the flue gas in a 330 MW coal-fired power plant. The pilot test achieved a good effect of flue gas dehydration. In previous studies, circulating water was mostly used as the ceramic membrane condenser cooling medium. However, the high circulating water temperature can seriously reduce the flue gas water and waste heat recovery effect. This paper tries to use the boiler secondary air as the ceramic membrane condenser cooling medium and realize the low-temperature waste heat effective recovery and utilization. As shown in Figure 1, the flue gas enters the ceramic membrane module after passing through the air preheater, the dust collector, and the wet desulfurization tower. As shown in Figure 1a, the porous ceramic membrane module often uses circulating water as the cooling medium. As shown in Figure 1b, by using the boiler secondary air instead of circulating water as the cooling medium, part of the water and waste heat in the flue gas is absorbed by the secondary air, and the secondary air is reheated by the air preheater and then sent into the boiler furnace. By initially heating the secondary air, the low-temperature corrosion problem on the flue gas side of the air preheater can be alleviated, and the low-temperature waste heat utilization problem can be solved. In this paper, with positive-pressure purge gas as the ceramic membrane condenser cooling medium, an experimental platform for water and waste heat recovery is established. A series of experimental



a) Circulating water as cooling medium



b) The secondary air as cooling medium

**Figure 1.** Ceramic membrane condenser recovering water and waste heat from flue gas.

investigations are carried out for water recovery characteristics, heat recovery characteristics, and purge gas outlet parameters.

## 2. EXPERIMENTAL SYSTEM AND METHODS

**2.1. Ceramic Membrane Module.** The ceramic membranes belong to porous media. As shown in Figure 2, there are

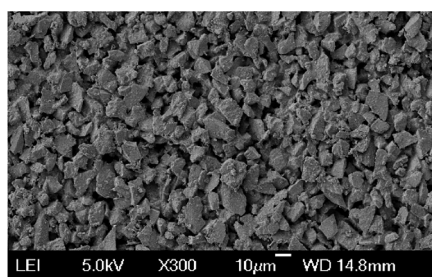


**Figure 2.** Ceramic membrane pore structure.

a large number of porous channels seen from an SEM (scanning electron microscope). The porous ceramic membrane is a single-channel structure, and it is composed of a hydrophilic alumina material.<sup>19,30</sup> The ceramic membrane pore sizes are 0.4 nm, 10 nm, 30 nm, 50 nm, and 1  $\mu\text{m}$ , and the porosity is between 31 and 34%. The ceramic membrane can be divided into symmetrical and asymmetrical types; moreover, the asymmetrical type can be divided into an outer coating and an inner coating. Among the above several membrane types,

the 1  $\mu\text{m}$  ceramic membrane is a symmetric structure, and the rest of the ceramic membranes are external coating structures. As shown in Figure 3, the purge gas and the flue gas in the

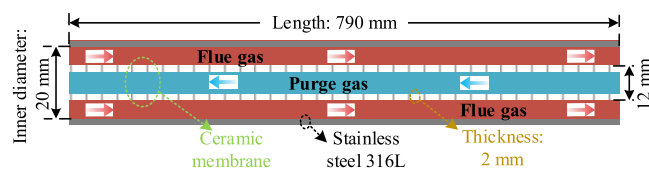
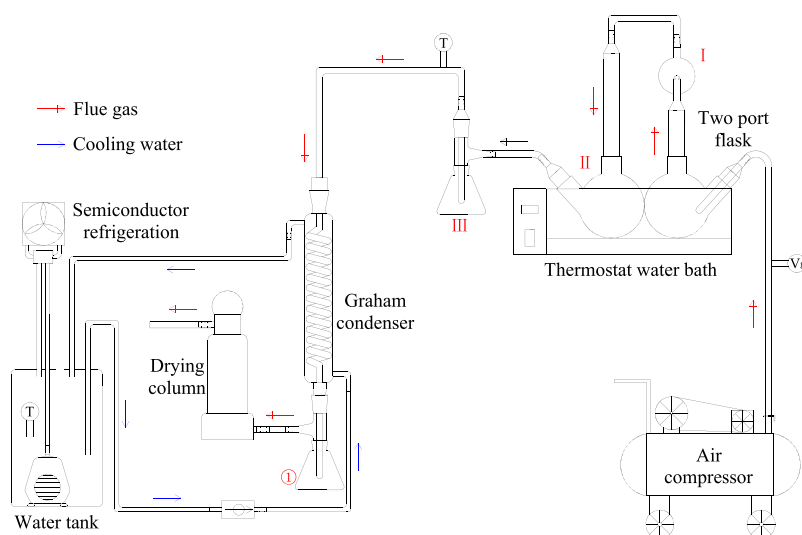


**Figure 3.** Ceramic membrane module.

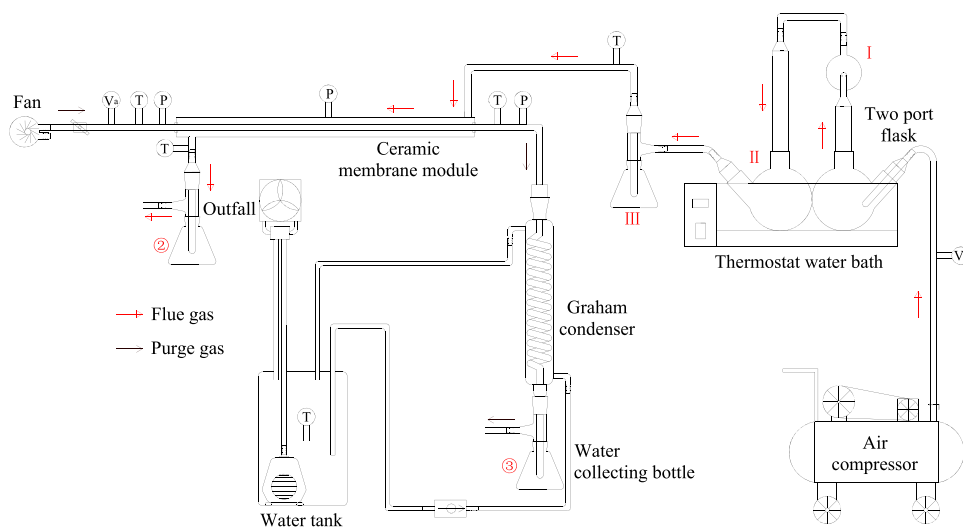
membrane module flow in the opposite direction.<sup>39</sup> The flue gas is located in the membrane module shell side, and the purge gas is located in the membrane module tube side. The membrane module shell is made of 316L stainless steel, and the membrane module shell inner diameter is 20 mm. The ceramic membrane tube has a length of 790 mm, an outer diameter of 12 mm, and a wall thickness of 2 mm.

**2.2. Experimental System.** In order to accurately obtain the water and waste heat recovery characteristics, it is necessary to accurately understand the flue gas moisture content in the ceramic membrane module inlet. As shown in Figure 4, during the experiment, the flue gas is replaced by air heating and humidification. The air compressor continuously supplies the dry flue gas, and the two-neck flask in the constant-temperature water bath is used to heat and humidify the dry flue gas. The devices I, II, and III are used to remove most of the liquid droplets carried by the flue gas stream. Figure 4a shows the flue gas moisture content measurement system, and it is used to accurately verify the flue gas supersaturation coefficient. The flue gas directly enters the serpentine condenser and the drying tower, so the water in the flue gas is removed by low-temperature condensation and solid adsorption. The flue gas moisture content can be determined by measuring the weight of the condensation water and the weight gain of the drying tower. Figure 4b shows the ceramic membrane condenser experimental platform for water and waste heat recovery from the flue gas. The purge gas fan is installed at the ceramic membrane module tube side inlet. The low-temperature condensation method is used to measure the purge gas moisture content. The water absorbed from the flue gas by the purge gas is collected and measured in conical bottle no. 3. Semiconductor cooling is used to maintain the cooling water tank temperature at 3–4  $^{\circ}\text{C}$ . The flue gas is discharged directly after the condensation water is collected by conical bottle no. 2 at the ceramic membrane module shell side outlet. Table 2 lists the experimental parameter range, including flue gas temperature, flue gas flow, purge gas flow, and ceramic membrane pore size.

The experimental platform is equipped with many measuring instruments. A metal tube rotor flowmeter is used to measure the dry flue gas volume flow, which is arranged at the air compressor outlet. A glass tube rotor flowmeter is used to measure the purge gas volume flow, which is arranged at the ceramic membrane module tube side inlet. The Pt100 thermocouples are used to measure the purge gas inlet and outlet temperature, which are arranged at the ceramic membrane module tube side inlet and outlet. Likewise, the Pt100 thermocouples are used to measure the flue gas inlet and outlet temperature, which are arranged at the ceramic membrane module shell side inlet and outlet. The diffusion silicon pressure transmitters are used to measure the purge gas



a) Measure the flue gas moisture content



b) Ceramic membrane condenser for water and waste heat recovery

Figure 4. Flue gas water and waste heat recovery experimental platform.

Table 2. Selection of Experimental Parameters

parameter	unit	value	parameter	unit	value
flue gas temperature	°C	38–64	flue gas flow	L/min	5.42/9.63/15.13
membrane pore size	nm	0.4/10/30/50/1000	purge gas flow	L/min	0–15

inlet and outlet pressure, which are arranged at the ceramic membrane module tube side inlet and outlet. Likewise, the diffusion silicon pressure transmitter is used to measure the flue gas pressure, which is arranged at the middle position of the ceramic membrane module shell side. The measurement range and uncertainty of instruments in the experimental platform are shown in Table 3. The above measuring instruments are provided by Beijing Zhongneng Boyu Technology Sensing Technology Co., Ltd.

Table 3. The Instrument Parameters in the Experimental Platform

instruments	model	range	uncertainty
metal rotor flowmeter	CGYL-LZ-25	0–30 L/min	0.3 L/min
glass rotor flowmeter	LZB-6WB	0–20 L/min	0.3 L/min
Pt100 thermocouple	SWB-B	0–100 °C	0.25 °C
pressure transmitter	CGYL-202	–50 to 50 kPa	0.25 kPa

**2.3. Heat and Mass Transport Model.** In the water and waste heat recovery process, the water vapor condenses and



releases the latent heat, so the synchronous recovery process of the flue gas water and waste heat is realized.<sup>40</sup> The water and waste heat recovery process is shown in Figure 5. First, the

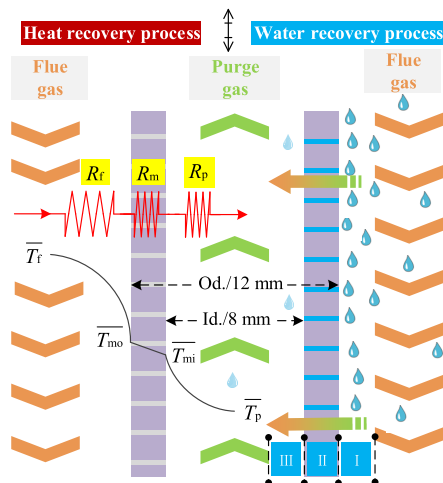


Figure 5. Heat and mass transport model.

water vapor undergoes film condensation on the ceramic membrane outer surface or capillary condensation in the ceramic membrane pore,<sup>17,26</sup> and the water vapor is converted into liquid water.<sup>27</sup> Then, part of the liquid water is transferred from the ceramic membrane outer surface to the ceramic membrane inner surface under the pressure difference. Finally, the liquid water on the ceramic membrane inner surface is converted from liquid water to water vapor by the humidity difference. Under the effect of forced flow and the temperature difference,<sup>29</sup> the heat transfer on the flue gas side includes convective heat transfer and conduction heat transfer. The heat transfer resistance mainly comes from factors such as the noncondensable gas boundary layer and the condensed water liquid film.<sup>32,34</sup> The heat transfer process is conduction heat transfer in the ceramic membrane tube wall, which is divided into two parts, condensed water and the ceramic membrane material.<sup>18,32,35</sup> The heat transfer on the purge gas side includes convective heat transfer and conduction heat transfer, and the heat transfer resistance mainly comes from the purge gas boundary layer.

**2.3.1. Water Recovery Characteristics.** The purge gas is used as the porous ceramic membrane condenser cooling medium to recover the water and waste heat from the flue gas. Common evaluation indicators for water recovery characteristics include the water recovery rate<sup>19</sup> and efficiency.<sup>34</sup>

$$v = \frac{3V}{50S\Delta t}$$

where  $v$  is the water recovery rate,  $L \cdot m^{-2} \cdot h^{-1}$ .  $S$  is the ceramic membrane outer surface area,  $297.67 \times 10^{-4} m^2$ .  $\Delta t$  is the operation time, min.  $V$  is the water volume of conical flask no. 3, mL.

In the ceramic membrane condenser, the theoretical water recovery flux can be calculated based on the difference between the flue gas inlet saturation moisture content and the flue gas outlet saturation moisture content. However, the actual water recovery flux can be measured by conical bottle no. 3. The ceramic membrane inside has a slightly positive pressure. In addition to recovering part of the condensation water by the ceramic membrane, there is still impermeable condensation water discharged from the ceramic membrane module with the flue gas. Considering the ceramic membrane's transmission characteristics for condensation water, there is a difference between the theoretical water recovery efficiency and actual water recovery efficiency. Taking into account the ceramic membrane transmission properties, the theoretical water recovery efficiency and ceramic membrane transmission efficiency are introduced:

$$\kappa = \frac{\alpha d_{T_i^s} - d_{T_o^s}}{\alpha d_{T_i^s}} \times 100$$

$$\theta = \frac{1000\rho_w V}{\Delta t V_g \rho_g (\alpha d_{T_i^s} - d_{T_o^s})} \times 100$$

$$\beta = \frac{1000\rho_w V}{\Delta t V_g \rho_g \alpha d_{T_i^s}} \times 100$$

where  $\kappa$ ,  $\theta$ ,  $\beta$  are the theoretical water recovery efficiency, the ceramic membrane transmission efficiency, and the actual water recovery efficiency, respectively, %.  $\alpha$  is the flue gas supersaturation coefficient, as shown in Table 4.  $d_{T_i^s}$  and  $d_{T_o^s}$  are the flue gas saturated moisture content at the ceramic membrane module inlet and outlet, respectively, g/kg (dry flue gas).  $\rho_w$  is the condensate water density, 1 g/mL.  $V_g$  is the dry flue gas volume flow, L/min.  $\rho_g$  is the dry flue gas density, 1.80 kg/m<sup>3</sup>.

**2.3.2. Heat Recovery Characteristics.** The waste heat recovery from the flue gas can be divided into the sensible heat recovery and the latent heat recovery.<sup>17,28</sup> The heat recovery power<sup>30</sup> and efficiency<sup>34</sup> were defined as follows:

$$Q_s = \frac{V_g \rho_g [(a d_{T_i^s} - d_{T_o^s})(T_i^s - T_o^s) C_p^w + 1000(T_i^s - T_o^s) C_p^s + (T_i^s - T_o^s) d_{T_i^s} C_p^{s,w}]}{6 \times 10^7}$$

$$Q_L = \frac{V_g \rho_g (d_{T_i^s} - d_{T_o^s}) r}{6 \times 10^4}$$

$$\Phi = Q_s + Q_L$$

$$\eta = \frac{6 \times 10^9 Q}{V_g \rho_g [1000 r d_{T_i^s} + a d_{T_i^s} (T_i^s - T_e) C_p^w + 1000(T_i^s - T_e) C_p^s]}$$

where  $\Phi$ ,  $Q_L$ , and  $Q_s$  are the heat recovery power, the latent heat recovery power, and the sensible heat recovery power, respectively, W.  $T_i^s$  and  $T_o^s$  are the flue gas inlet and outlet temperature in the ceramic membrane module, respectively, °C.  $C_p^w$  is the specific heat capacity of water, 4200 J/kg/K.  $C_p^s$  is the specific heat capacity of dry flue gas, 1007 J/kg/K.  $C_p^{s,w}$  is

Table 4. Flue Gas Moisture Content Supersaturation Coefficient

flue gas flow	testing times	supersaturation coefficient	flue gas flow	testing times	supersaturation coefficient
4.75 L/min	11	1.41	15.20 L/min	10	1.07
9.47 L/min	11	1.24	19.83 L/min	11	1.04

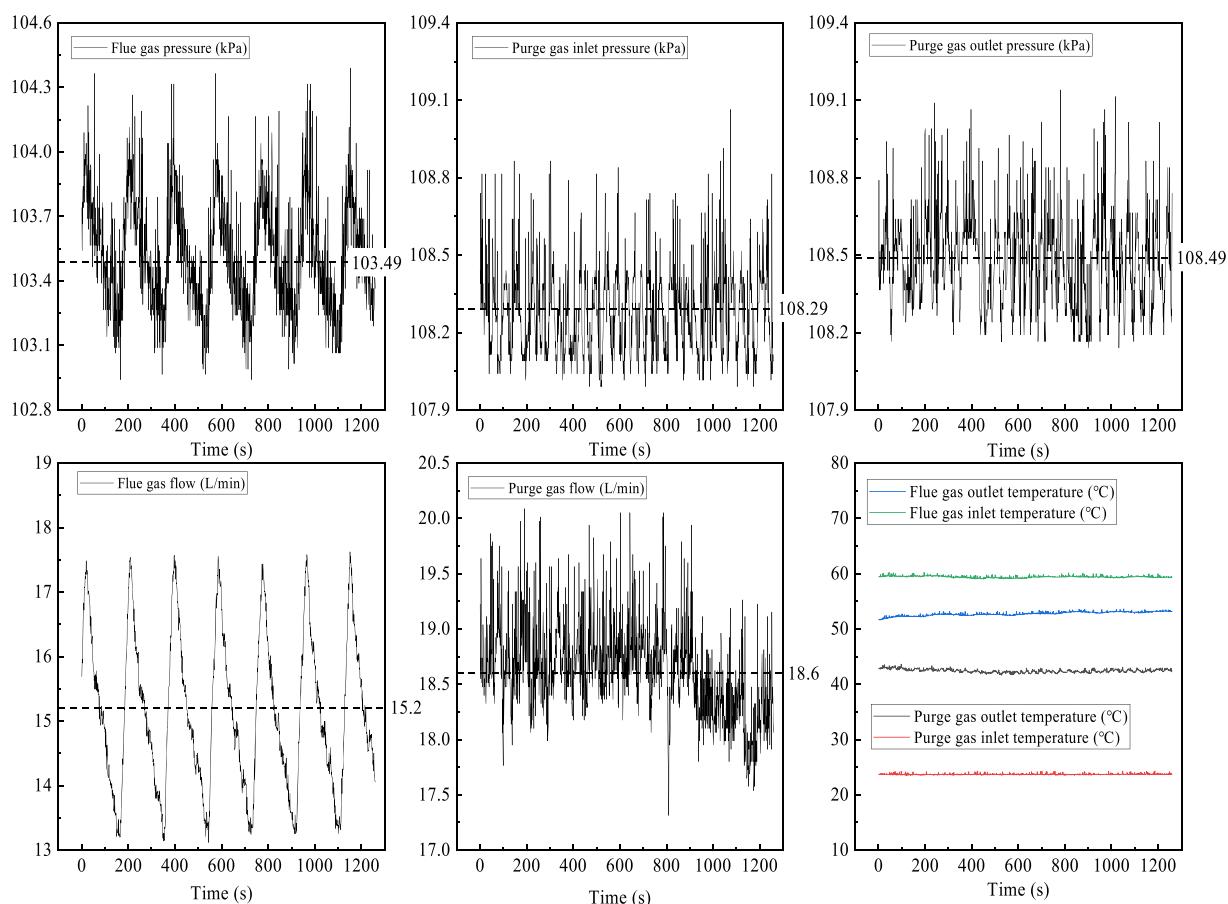


**Figure 6.** Running state parameters (experimental conditions: flue gas flow, 15.2 L/min; flue gas temperature, 59.4 °C; purge gas flow, 18.6 L/min; purge gas temperature, 23.7 °C; ceramic membrane pore size, 10 nm).

the specific heat capacity of water vapor, 1871 J/kg·K.  $r$  is the water vapor latent heat, 2257 kJ/kg.  $T_e$  is the ambient temperature, °C.

**2.3.3. Purge Gas Outlet Characteristics.** The purge gas absorbs the water and waste heat from the flue gas, and the purge gas temperature and moisture content are significantly increased. In order to characterize the purge gas outlet characteristic parameters, the following indicators are defined:

$$d_p = \frac{1000\rho_w V}{\Delta t V_a \rho_a}$$

$$\varphi = \frac{d_p}{d_s}$$

where  $d_p$  is the purge gas outlet moisture content, g/kg.  $V_a$  is the purge gas volume flow, L/min.  $\rho_a$  is the purge gas density, kg/m<sup>3</sup>.  $\varphi$  is the purge gas outlet relative humidity, %.  $d_s$  is the saturated moisture content at the purge gas outlet temperature, g/kg.

**2.3.4. Heat Transfer Resistance.** The ceramic membrane recovers the waste heat from the flue gas, and the heat transfer resistance is composed of four parts in series,<sup>39</sup> which are the liquid film thermal resistance, the noncondensable gas boundary layer thermal resistance, the ceramic membrane tube wall thermal resistance, and the purge gas boundary layer thermal resistance.<sup>25,41</sup> The ceramic membrane tube wall is composed of the ceramic membrane material and condensation water. The Biot number, which is used to analyze the

relationship between the ceramic membrane tube wall thermal resistance and the external thermal resistance, will help to understand the ceramic membrane module heat transfer characteristics.<sup>32,34</sup>

$$R = R_f + R_m + R_p$$

$$\lambda = (1 - \phi)\lambda_m + \phi\lambda_w$$

$$\frac{\Phi}{l} = \frac{\bar{T}_f - \bar{T}_p}{R_f + R_m + R_p}$$

$$R_m = \frac{\ln(12/8)}{2\pi\lambda} \Rightarrow \frac{0.20}{\pi\lambda}$$

$$B_i = \frac{h\delta}{\lambda} \Rightarrow \frac{R_m}{R_f + R_p}$$

where  $\lambda$  is the ceramic membrane tube wall thermal conductivity, W·m<sup>-1</sup>·K<sup>-1</sup>;  $\lambda_m$  is the ceramic membrane material thermal conductivity, W·m<sup>-1</sup>·K<sup>-1</sup>;  $\lambda_w$  is the condensation water thermal conductivity, W·m<sup>-1</sup>·K<sup>-1</sup>;  $\phi$  is the ceramic membrane porosity, %;  $R_f$  is the heat transfer resistance on the flue gas side, m<sup>2</sup>·K·W<sup>-1</sup>;  $R_m$  is the heat transfer resistance on the ceramic membrane tube wall, m<sup>2</sup>·K·W<sup>-1</sup>;  $R_p$  is the heat transfer resistance on the purge gas side;  $l$  is the ceramic membrane tube length;  $\bar{T}_f$  and  $\bar{T}_p$  are the flue gas average temperature and purge gas average temperature, respectively, °C;  $\delta$  is the ceramic membrane tube wall effective thickness, m;  $h$  is the

ceramic membrane tube wall external heat transfer coefficient,  $\text{W}\cdot\text{m}^{-2}\cdot\text{K}^{-1}$ .

### 3. RESULTS AND DISCUSSION

The experimental system runs continuously for 21 min, and the state parameters are shown in Figure 6. The air compressor working principle determines that the flue gas flow and pressure present regular fluctuations. The local atmosphere pressure is 102.19 kPa. The flue gas average flow is 15.2 L/min, and the flue gas average pressure is 103.49 kPa. The purge gas absorbs the water and waste heat from the flue gas in the ceramic membrane module, which causes the purge gas temperature and moisture content increase. The purge gas inlet and outlet average pressures are 108.29 and 108.49 kPa. The ceramic membrane module has 4 points for temperature measurement. The temperature is relatively stable during operation. The flue gas inlet temperature is 59.4 °C. The flue gas outlet temperature is 52.8 °C. The purge gas inlet temperature is 23.7 °C. The purge gas outlet temperature is 42.4 °C. The order of each temperature from the largest to the smallest is  $T_{\text{f}}^{\text{s}} > T_{\text{f}}^{\text{a}} > T_{\text{p}}^{\text{a}} > T_{\text{p}}^{\text{s}}$ .

#### 3.1. Water and Heat Recovery Characteristics.

##### 3.1.1. Effect of Flue Gas Temperature. Figure 7 shows the

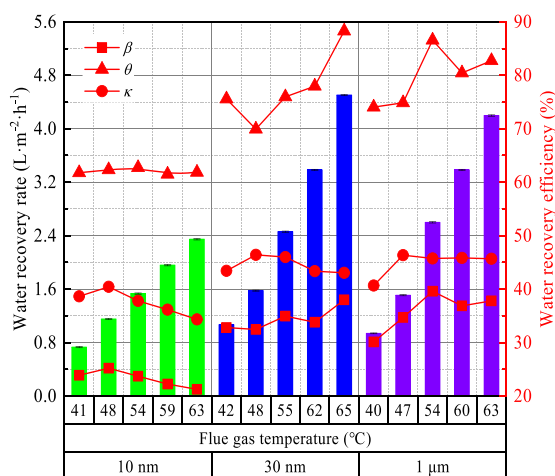


**Figure 7.** Water recovery rate/efficiency vs flue gas temperature (experimental conditions: flue gas flow, 15.25 L/min; purge gas flow, 18 L/min; purge gas temperature, 12.95 °C; ceramic membrane pore size, 10 nm/30 nm/1 μm).

water recovery rate and efficiency with flue gas temperature. The water recovery rate shows a continuous increasing trend with the flue gas temperature increases. For instance, in the 30 nm ceramic membrane module, the flue gas temperature increases from 42 to 65 °C, and the corresponding water recovery rate increases from 1.1 to 4.5  $\text{L}\cdot\text{m}^{-2}\cdot\text{h}^{-1}$ . This paper has the same change trend with the literature.<sup>24,30</sup> However, when the flue gas temperature is 65 °C, the maximum water recovery rate is only 2  $\text{L}/\text{h}/\text{m}^2$  in the literature.<sup>24</sup> The water recovery rate is higher in this paper because the flue gas flow is higher in the experimental condition. For the wet saturated flue gas, the flue gas temperature is higher, and the flue gas moisture content and the water vapor partial pressure are higher.<sup>29</sup> Therefore, the above changes contribute to the water vapor condensation of the flue gas side, transmission in the ceramic membrane wall, and liquid water evaporation of the purge gas side. Under the experimental conditions, increasing

the flue gas temperature by 23 °C can increase the water recovery rate by 3–5 times. However, for the 30 nm ceramic membrane module, the theoretical water recovery rate is 43–47%, and the actual water recovery efficiency is only 32–38%. There is a big difference between the theoretical and the actual water recovery efficiency. Because some condensation water is not effectively recovered by the ceramic membrane, it is directly discharged from the membrane module with the flue gas. In the literature,<sup>25,26</sup> the water recovery efficiency is obtained by calculating the flue gas inlet and outlet saturated moisture content in the membrane module. Based on the literature,<sup>25,26</sup> the actual water recovery efficiency and the ceramic membrane transmission efficiency are discussed in this paper. The ceramic membrane transmission efficiency is an important factor resulting in the difference between the actual water recovery efficiency and the theoretical water recovery efficiency. In the 30 nm ceramic membrane module, the theoretical water recovery efficiency decreases, while the actual water recovery efficiency increases because the ceramic membrane transmission efficiency increases with increasing flue gas temperature.

Figure 8 shows the heat recovery power and efficiency with flue gas temperature. With the flue gas temperature increases,

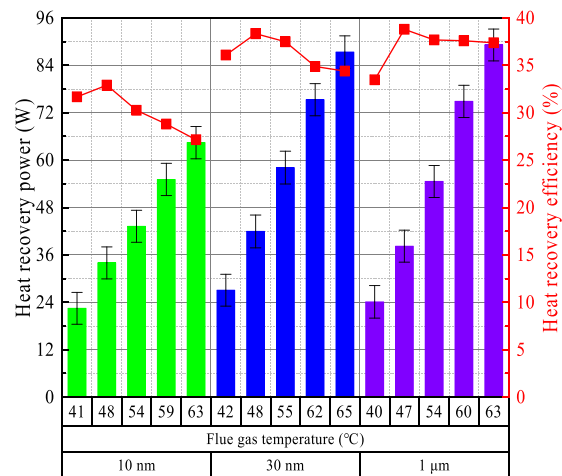


**Figure 8.** Heat recovery power/recovery efficiency vs flue gas temperature (experimental conditions: flue gas flow, 15.25 L/min; purge gas flow, 18 L/min; purge gas temperature, 12.95 °C; ceramic membrane pore size, 10 nm/30 nm/1 μm).

the heat recovery power significantly increases. For the 1 μm ceramic membrane module, the flue gas temperature increases from to 63 °C, and the corresponding heat recovery power increases from 24.1 to 89.2 W. The same results are reported in the literature.<sup>30</sup> With increasing the flue gas temperature, the heat transfer temperature difference is increased, which means that the heat transfer driving force is enhanced.<sup>29</sup> Moreover, the wet saturated flue gas temperature is higher, the flue gas moisture content is also larger, more water vapor releases latent heat, and the phase change heat process is enhanced. The heat recovery efficiency increases and then decreases, and the highest heat recovery efficiency is 39%. The literature<sup>30</sup> demonstrates the same trend for heat recovery efficiency; however, the overall heat recovery efficiency is low in this paper because in the literature,<sup>30</sup> circulating water as a relatively ceramic membrane module cooling medium has a relatively large specific heat capacity and has a relatively strong cooling

capacity. When the flue gas temperature increases at the initial stage, the total heat input to the membrane module is relatively small; thus, the heat recovery efficiency increases. However, when the flue gas temperature continues to increase, the total heat input to the ceramic membrane module will increase significantly. Increasing the condensation water liquid film thermal resistance formed by water vapor condensation leads to a lower increase in heat recovery power than the total heat input increase in the ceramic membrane module. Moreover, the heat discharged with the flue gas will increase faster, which will inevitably lead to a decrease in heat recovery efficiency. The same reason is given in the literature.<sup>30</sup> Compared with the literature,<sup>25</sup> the heat recovery efficiency is lower in this paper because the cooling medium is water in the literature,<sup>25</sup> while the cooling medium is purge gas in this paper.

**3.1.2. Effect of Purge Gas Flow.** The ceramic membrane condenser recovers the water from the flue gas with purge gas as the cooling medium. The purge gas pressure is higher than the flue gas pressure in the ceramic membrane module. The purge gas flow is higher; the purge gas pressure is higher. Figure 9 shows the variation in the water recovery rate and

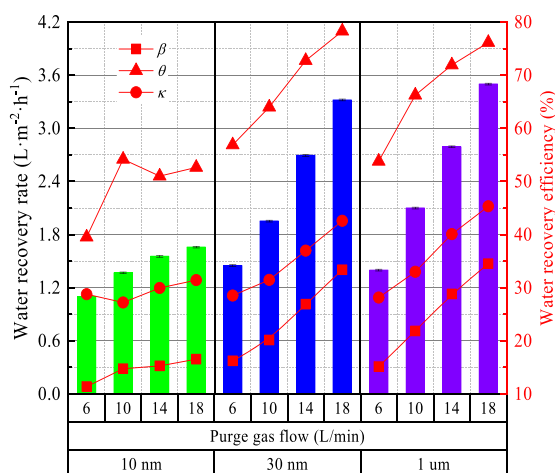


**Figure 9.** Water recovery rate/efficiency vs purge gas flow (experimental conditions: flue gas flow, 15.17 L/min; flue gas temperature, 60.92 °C; purge gas temperature, 22.92 °C; ceramic membrane pore size, 10 nm/30 nm/1 μm).

efficiency with purge gas flow. The water recovery rate increases with the purge gas flow increases. For instance, in the 30 nm ceramic membrane module, the purge gas flow has increased from 6 to 18 L/min, and the corresponding water recovery rate has increased from 1.5 to 3.3 L·m<sup>-2</sup>·h<sup>-1</sup>. Similarly, in the 1 μm ceramic membrane module, the purge gas flow has increased from 6 to 18 L/min, and the corresponding water recovery rate has increased from 1.4 to 3.5 L·m<sup>-2</sup>·h<sup>-1</sup>. The higher purge gas flow has a higher flue gas cooling capacity. In the literature,<sup>37</sup> circulating water is used as the ceramic membrane module cooling medium, and the water recovery rate likewise increases with the cooling medium flow increases. The theoretical water recovery efficiency, ceramic membrane transmission efficiency, and actual water recovery efficiency also increase with the purge gas flow increases. The theoretical water recovery efficiency and the actual water recovery efficiency also have a big difference. As shown in Figure 10, the heat recovery power and efficiency change trend with the purge gas flow is basically the same as the water

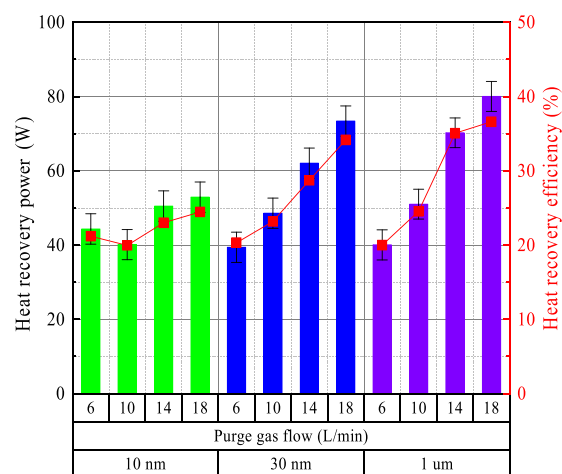


**Figure 10.** Heat recovery power/efficiency vs purge gas flow (experimental conditions: flue gas flow, 15.17 L/min; flue gas temperature, 60.92 °C; purge gas temperature, 22.92 °C; ceramic membrane pore size, 10 nm/30 nm/1 μm).

recovery characteristics. The literature<sup>34</sup> also shows that increasing the cooling medium flow helps to increase the water recovery rate and the heat recovery power. With the purge gas flow increases from 6 to 18 L/min, the heat recovery power increases by nearly 2 times, and the heat recovery efficiency increases by nearly 37%. The change trends of 1 μm and 30 nm ceramic membrane modules are more obvious than the change trend of the 10 nm ceramic membrane module. Increasing the purge gas flow can reduce the purge gas average temperature and increase the heat transfer temperature difference. On the other hand, a higher purge gas flow corresponds to a reduction in the noncondensable gas boundary layer thickness.

**3.1.3. Effect of Membrane Pore Size.** The ceramic membrane pore size also has a certain effect on the water and waste heat recovery characteristics.<sup>42</sup> The experimental conditions are shown in Table 5. The random selection of

**Table 5. The Experimental Conditions for Different Ceramic Membrane Pore Sizes**

	flue gas temperature	flue gas flow	purge gas temperature	purge gas flow
condition 1	57.94 °C	5.42 L/min	17.19 °C	15 L/min
condition 2	56.53 °C	9.63 L/min	16.24 °C	13 L/min
condition 3	61.54 °C	15.13 L/min	22.95 °C	18 L/min

three different experimental conditions helps to increase the confidence of the analysis results. Based on different experimental conditions, Figure 11 shows the water recovery rate and efficiency with different ceramic membrane pore sizes. It can be found that the 0.4 nm ceramic membrane water recovery rate and efficiency are far lower than the other ceramic membranes' water recovery rate and efficiency. In the literature,<sup>43</sup> negative-pressure air is used as the cooling medium, and the 0.4 nm ceramic membrane water recovery characteristics are also similarly poor. The 0.4 nm ceramic membrane is not suitable for the flue gas dehydration process. Under experimental conditions 1 and 2, the flue gas flow is low, and the 10 nm and 1 μm ceramic membranes' water recovery rate and efficiency are relatively small. Under experimental condition 3, the flue gas flow is high, and the



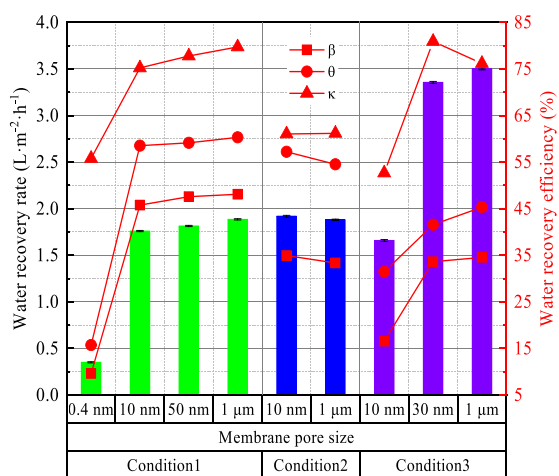


**Figure 11.** Water recovery rate/efficiency vs ceramic membrane pore size.

10 nm ceramic membrane water recovery rate and efficiency are lower than the 1  $\mu\text{m}$  ceramic membrane water recovery rate and efficiency. When the flue gas flow is high, the condensation water residence time in the membrane module is short and the condensation water transmission efficiency is weakened. The ceramic membrane has a smaller pore size, resulting in a larger liquid film thickness on the flue gas side, and has a lower water recovery efficiency.

Under the same experimental conditions, Figure 12 shows the effects of ceramic membranes' pore sizes on heat recovery

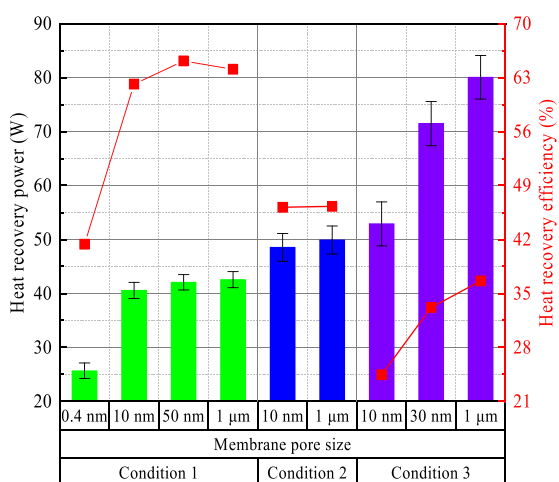
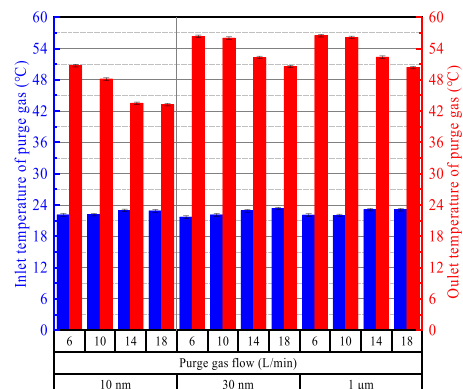


**Figure 12.** Heat recovery power/efficiency vs ceramic membrane pore size.

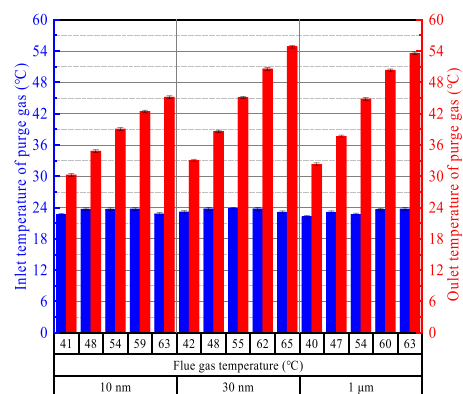
power and efficiency. Under experimental condition 1, the 0.4 nm ceramic membrane heat recovery power and efficiency are relatively small. The 0.4 nm pore size is too small, causing a large amount of condensation water to form a liquid film on the flue gas side, increasing the heat transfer resistance. Under experimental condition 2, the 10 nm and 1  $\mu\text{m}$  ceramic membranes' heat recovery power and efficiency are basically the same. Under experimental condition 3, with the ceramic membrane pore size increases, the heat recovery power and efficiency are significantly improved. When the flue gas temperature and flow are high, the flue gas moisture content is also high and the large pore size ceramic membrane helps

condensation water to be transported across the membrane tube wall and reduces the liquid film thermal resistance on the flue gas side.

**3.2. Purge Gas Characteristics.** The purge gas is used as the cooling medium in the ceramic membrane condenser, and the temperature is significantly increased after absorbing the waste heat from the flue gas. As shown in Figure 13, the purge



**a)** Inlet (Outlet) temperature of purge gas vs. Purge gas flow

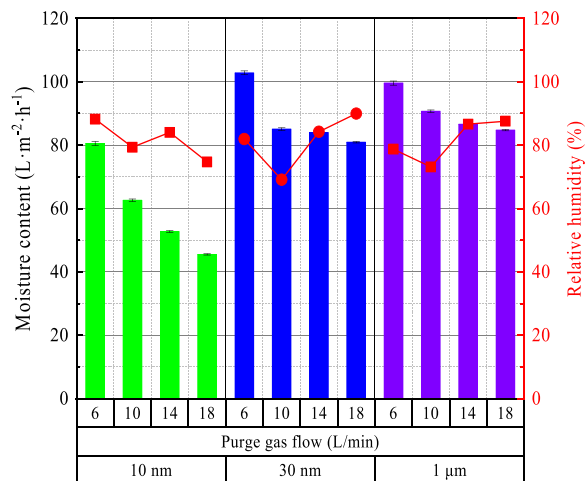


**b)** Inlet (Outlet) temperature of purge gas vs. Flue gas temperature

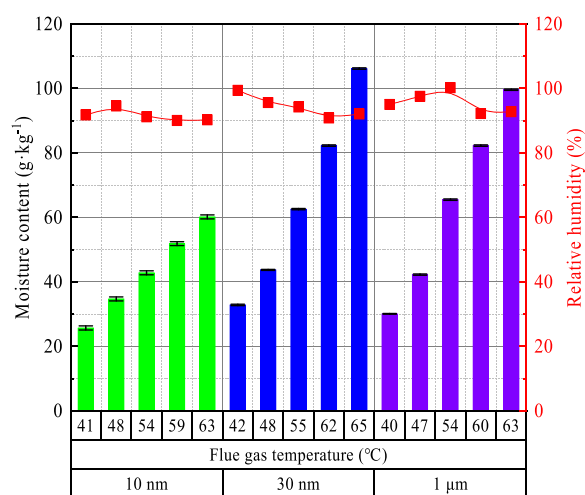
**Figure 13.** Purge gas inlet/outlet temperature. (a) Experimental conditions: flue gas flow, 15.17 L/min; flue gas temperature, 60.92  $^{\circ}\text{C}$ ; membrane pore size, 10 nm/30 nm/1  $\mu\text{m}$ . (b) Experimental conditions: flue gas flow, 15.25 L/min; purge gas flow, 18 L/min; membrane pore size, 10 nm/30 nm/1  $\mu\text{m}$ .

gas outlet temperature is significantly higher than the purge gas inlet temperature. As shown in Figure 13a, the purge gas outlet temperature shows a slightly decreasing trend. Increasing the purge gas flow expands the flue gas waste heat recovery capacity and reduces the noncondensable gas boundary layer thickness on the purge gas side. However, increasing the purge gas flow leads to the purge gas residence time decrease in the ceramic membrane module and lowers the purge gas outlet temperature. In Figure 13b, the purge gas outlet temperature continues to increase rapidly with the flue gas temperature increases. Increasing the flue gas temperature, on the one hand, helps to increase the flue gas waste heat input of the ceramic membrane module. On the other hand, it significantly increases the ceramic membrane module heat exchange temperature difference, so the purge gas outlet temperature changes more with the flue gas temperature.

The purge gas moisture content is mainly affected by the water recovery rate and the purge gas flow. The main influencing factors of relative humidity include the purge gas moisture content and the temperature. This experiment mainly studied the effects of purge gas flow, flue gas temperature, and ceramic membrane pore size on the purge gas moisture content. As shown in Figure 14a, with the purge gas flow



a) Purge gas flow



b) Flue gas temperature

**Figure 14.** Purge gas moisture content/relative humidity. (a) Experimental conditions: flue gas flow, 15.17 L/min; flue gas temperature, 60.92 °C; purge gas temperature, 22.92 °C; membrane pore size, 10 nm/30 nm/1 μm. (b) Experimental conditions: flue gas flow, 15.25 L/min; purge gas flow, 18 L/min; purge gas temperature, 23.41 °C; membrane pore size, 10 nm/30 nm/1 μm.

increases, the purge gas moisture content continues to decrease. Moreover, the purge gas relative humidity also decreases with the purge gas flow increases in the 10 nm ceramic membrane module. However, in the 30 nm and 1 μm ceramic membrane modules, the purge gas relative humidity decreases first and then increases with the purge gas flow increases. Increasing purge gas flow will reduce the purge gas outlet temperature. Compared with the 30 nm and 1 μm ceramic membrane modules, the purge gas moisture content decreases significantly in the 10 nm ceramic membrane

module, resulting in a continuous decrease in the relative humidity. Figure 14b shows the effect of flue gas temperature on the purge gas moisture content. When the flue gas temperature increases, the purge gas moisture content increases significantly. The wet saturated flue gas with a higher temperature helps to increase the water recovery rate, resulting in an increase in the purge gas moisture content. With increasing the flue gas temperature, the purge gas outlet temperature and moisture content both increase significantly, resulting in a relatively stable relative humidity. The purge gas relative humidity is stable within the range of 90–100%. In contrast, the purge gas relative humidity was higher than 100% in the literature.<sup>43</sup> The reason is that the purge gas has a negative pressure in the literature,<sup>43</sup> while the purge gas has a positive pressure in this paper. The negative-pressure condition in the ceramic membrane is favorable for the condensation water transmission across the membrane.

**3.3. Heat Transfer Resistance Characteristics.** The ceramic membrane condenser is used to recover the waste heat from the flue gas, and the heat transfer resistance can be divided into the ceramic membrane tube wall heat transfer resistance and the ceramic membrane inner and outer surfaces' heat transfer resistance.<sup>41</sup> The Biot number represents the ratio of the ceramic membrane tube wall thermal resistance and the external thermal resistance. Since the ceramic membrane tube wall thermal resistance includes the membrane material thermal resistance and the condensation water thermal resistance, so, it is basically unchanged.<sup>18,32,35</sup> As shown in Figure 15, the Biot number increases with the flue gas

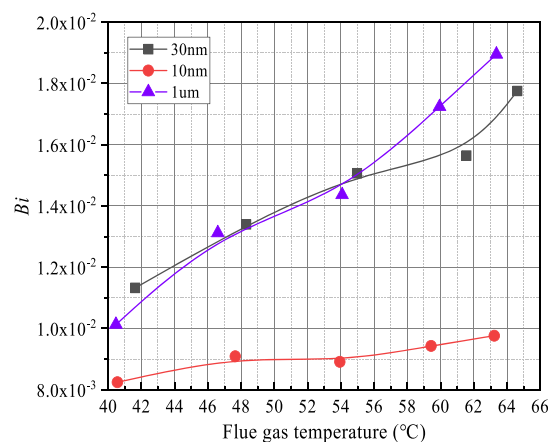
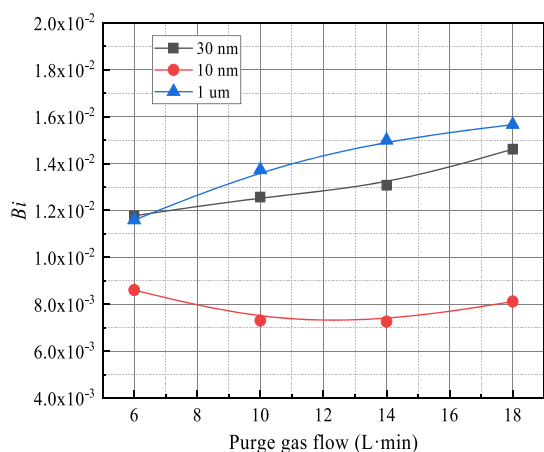
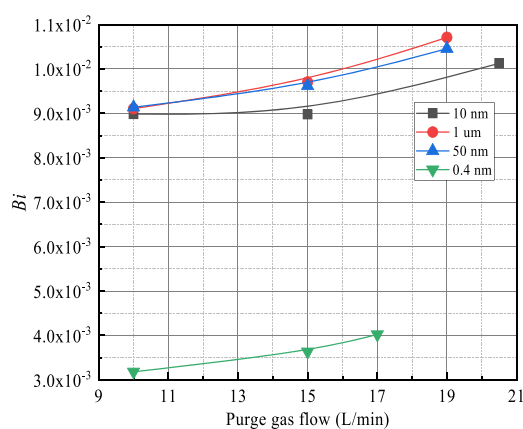


**Figure 15.** Bi vs flue gas temperature (experimental conditions: flue gas flow, 15.25 L/min; purge gas flow, 18 L/min; purge gas temperature, 23.41 °C; membrane pore size, 10 nm/30 nm/1 μm).

temperature increases. The wet saturated flue gas temperature is higher; the phase change heat capacity is higher per unit temperature difference. The highly efficient phase heat transfer capability reduces the heat transfer thermal resistance on the ceramic membrane inner and outer surfaces. At the same time, the Biot number of the 10 nm ceramic membrane is relatively small because the small ceramic membrane pore size limits the water transmission, which weakens the phase change heat in the purge gas side and increases liquid film thickness in the flue gas side. Figure 16 shows a slight increase in the Biot number with the purge gas flow increases because increasing the purge gas flow helps to enhance the purge gas phase change heat process. The Biot number of the 0.4 nm ceramic membrane is



a) High flue gas flow



b) Low flue gas flow

**Figure 16.** *Bi* vs purge gas. (a) Experimental conditions: flue gas flow, 15.17 L/min; flue gas temperature, 60.92 °C; purge gas temperature, 22.92 °C; membrane pore size, 10 nm/30 nm/1 μm. (b) Experimental conditions: flue gas flow, 5.41 L/min; flue gas temperature, 57.86 °C; purge gas temperature, 17.14 °C; membrane pore size, 0.4 nm/10 nm/50 nm/1 μm.

only 1/3 of the Biot numbers of other ceramic membranes with different pore sizes. The 0.4 nm ceramic membrane has a weaker transmission efficiency for condensation water, which increases the liquid film thickness on the flue gas side. Moreover, the phase change heat process is weakened in the purge gas side, so the ceramic membrane inner and outer surfaces' thermal resistance increases. From the above research, it is found that the ceramic membrane condenser with purge gas recovers the waste heat from the flue gas, and the Biot number is between  $3.2 \times 10^{-3}$  and  $1.9 \times 10^{-2}$ . The main thermal resistance limiting the heat recovery capacity comes from the flue gas side and the purge gas side, and the ceramic membrane tube wall thermal resistance is negligible. The literature<sup>25</sup> also obtains the same experimental conclusion. In the literature,<sup>25</sup> the ceramic membrane tube wall conductive resistance makes up only about 1% of the total thermal resistance. Comparing Figure 16a and b, it can be found that increasing the flue gas flow can reduce the ceramic membrane inner and outer surfaces' thermal resistance.

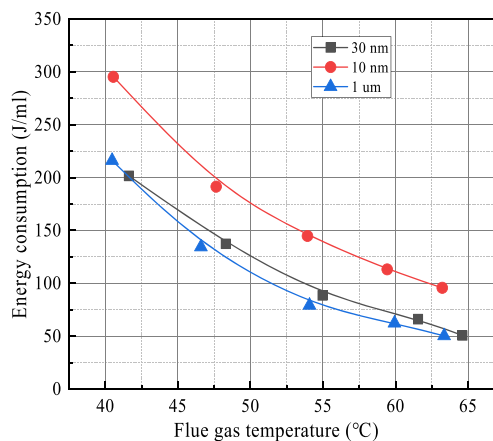
**3.4. Energy Consumption of Water Recovery.** Based on the experimental platform, the purge gas energy

consumption in the ceramic membrane condenser is analyzed. The energy consumption required for the purge gas can be obtained by analyzing the purge gas flow and pressure.

$$\omega = \frac{\Delta t V_p P_p^i}{\eta V}$$

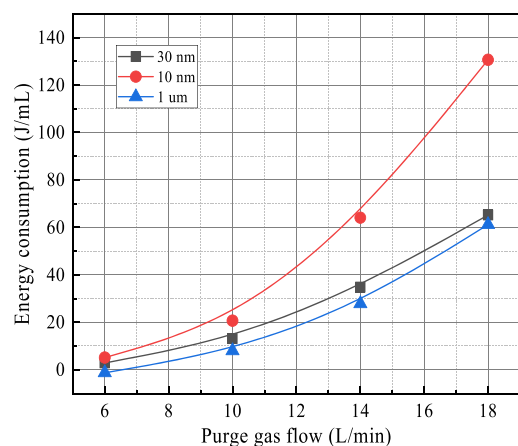
where  $\omega$  is the energy consumption of the fan for recovery unit volume condensation water, J/mL;  $P_p^i$  is the purge gas inlet pressure in the ceramic membrane module tube side, kPa;  $\eta$  is the purge gas fan efficiency, 100%. This experimental process focuses on the purge gas energy consumption in the ceramic membrane module, and the fan efficiency is assumed to be 100%.

Figure 17 illustrates the variation of purge gas energy consumption with flue gas temperature. The energy con-

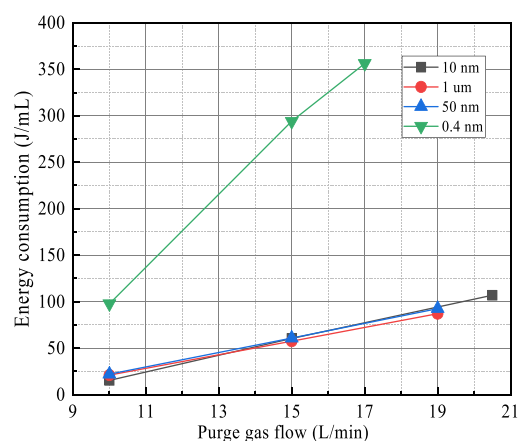


**Figure 17.** Energy consumption vs flue gas temperature (experimental conditions: flue gas flow, 15.25 L/min; purge gas flow, 18 L/min; purge gas temperature, 23.41 °C; membrane pore size, 10 nm/30 nm/1 μm).

sumption is relatively small for high flue gas temperatures, and the 10 nm ceramic membrane module has the highest energy consumption among the three different ceramic membrane modules. In the 10 nm ceramic membrane module, when the flue gas temperature increases from 40.6 to 63.2 °C, the corresponding purge gas energy consumption decreases from 295.2 to 95.7 J/mL because increasing the flue gas temperature helps to improve the water recovery rate. Thus, the energy consumption is relatively small under a certain purge gas flow. With the 10 nm ceramic membrane module, due to the relatively low water recovery rate, the purge gas energy consumption is relatively high. At the same temperature, the purge gas energy consumption in the 10 nm ceramic membrane module is higher than that in the 1 μm ceramic membrane module by 45–69 J/mL. Figure 18 shows that as the purge gas flow increases, the purge gas energy consumption also increases. Increasing the purge gas flow can increase the water recovery rate, but increasing the purge gas flow leads to an increase in the energy consumption of the fan. When the flue gas flow is high, the energy consumption of the 10 nm ceramic membrane module is higher than the energy consumption of the 1 μm ceramic membrane module, and with the purge gas flow increases, the difference continues to expand. When the flue gas flow is low, the energy consumption of the 10 nm ceramic membrane module is basically the same as the energy consumption of the 1 μm ceramic membrane.



a) High flue gas flow



b) Low flue gas flow

**Figure 18.** Energy consumption vs purge gas flow. (a) Experimental conditions: flue gas flow, 15.17 L/min; flue gas temperature, 60.92 °C; purge gas temperature, 22.92 °C; membrane pore size, 10 nm/30 nm/1 μm. (b) Experimental conditions: flue gas flow, 5.41 L/min; flue gas temperature, 57.86 °C; purge gas temperature, 17.14 °C; membrane pore size, 0.4 nm/10 nm/50 nm/1 μm.

The energy consumption is too high in the 0.4 nm ceramic membrane module, which again shows that it is not suitable for flue gas dehydration.

In the engineering application process, the boiler secondary air is used as the cooling medium in the ceramic membrane module. On the basis of the original blower, additional fans and cooling systems can be avoided. Therefore, the high energy consumption problem of water recovery can be effectively solved. The literature<sup>44</sup> investigated the economics of flue gas water recovery and found that the membrane separation method has the significant advantage.

### 3.5. Ceramic Membrane Module Entropy Generation.

Considering that the purge gas temperature is lower than the flue gas temperature, there is an obvious heat transfer temperature difference, so the ceramic membrane module entropy generation is caused by an irreversible process. The ceramic membrane module entropy production value can be determined by the following formula:

$$\Delta S = \Phi \left( \frac{1}{T_p} - \frac{1}{T_g} \right)$$

where  $\Delta S$  is the ceramic membrane module entropy production value per unit time, J/K.

As shown in Figure 19, the ceramic membrane module entropy production value increases significantly with the flue

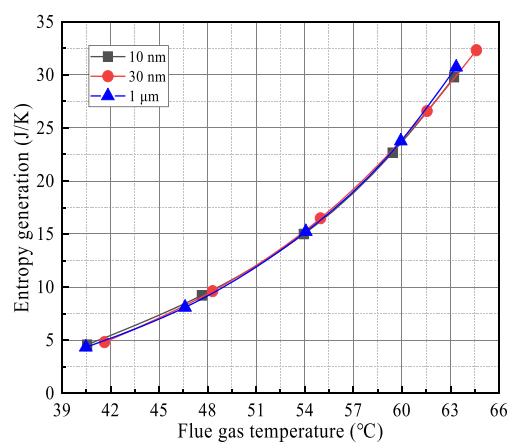


**Figure 19.** Entropy generation vs flue gas temperature (experimental conditions: flue gas flow, 15.25 L/min; purge gas flow, 18 L/min; purge gas temperature, 23.41 °C; ceramic membrane pore size, 10 nm/30 nm/1 μm).

gas temperature increases. Because the higher flue gas temperature corresponds to the higher heat recovery power, the heat exchange temperature difference also increases, which intensifies the irreversibility process of the ceramic membrane module. Figure 20 shows the effect of the ceramic membrane

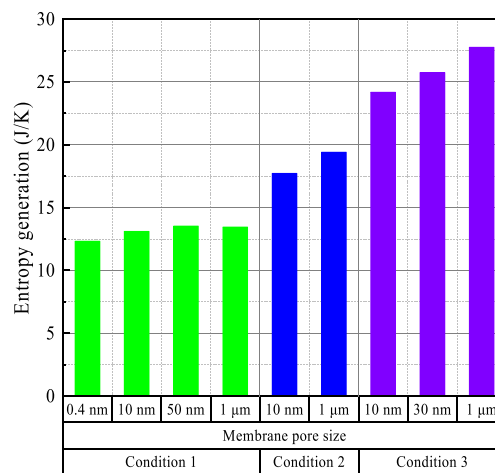


**Figure 20.** Entropy generation vs ceramic membrane pore size.

pore size on the ceramic membrane module entropy production value. The same experimental conditions are shown in Table 4. When the flue gas flow is 5.42 L/min, the entropy generation values of the 0.4 nm, 10 nm, 50 nm, and 1 μm ceramic membrane modules are basically the same, about 12.5 J/K. With the flue gas flow increases, the ceramic membrane module entropy production value increases with the membrane pore size increases. When the flue gas flow is 15.13 L/min, the flue gas temperature is 61.54 °C, the purge gas flow



is 18 L/min, and the purge gas temperature is 22.95 °C, the 1  $\mu\text{m}$  ceramic membrane module entropy production value is the largest, which is 27.8 J/K.

#### 4. CONCLUSIONS

The purge gas is used as the cooling medium of the ceramic membrane condenser, and an experimental platform for the water and waste heat recovery from flue gas is built. The flue gas temperature or purge gas flow is the key factor that affects the water and waste heat recovery characteristics. Increasing the purge gas flow promotes the water recovery rate and efficiency and heat recovery power and efficiency. Increasing the flue gas temperature can increase the water recovery rate and heat recovery power, but it cannot continue to increase the water recovery efficiency and heat recovery efficiency. Since the purge gas operates under a slightly positive pressure, except for the 0.4 nm ceramic membrane, the ceramic membrane transmission efficiency can range from 39 to 89%. Thus, there is a large difference between the actual water recovery efficiency and theoretical water recovery efficiency, which can be up to 31%. Under the experimental conditions, the Biot number of the ceramic membrane module is between  $3.2 \times 10^{-3}$  and  $1.9 \times 10^{-2}$ , and the ceramic membrane tube wall heat transfer resistance can be basically ignored.

The purge gas absorbs the water and waste heat from the flue gas. Under experimental conditions, the purge gas outlet temperature ranges from 30.3 to 56.5 °C, and the purge gas relative humidity ranges from 69.1 to 100%. Under the experimental platform, the energy consumption of water recovery is relatively large. By increasing the flue gas temperature, the energy consumption of water recovery can be reduced. At the same time, due to the certain heat exchange temperature difference between the flue gas and the purge gas, the ceramic membrane module entropy production value caused by the irreversible process increases with the flue gas temperature increases. The actual water recovery efficiency of the 0.4 nm ceramic membrane is about 10%, and it is too low to be suitable for the flue gas dehydration process. The 1  $\mu\text{m}$  ceramic membrane has excellent water and waste heat recovery characteristics. The above research results confirm that the boiler secondary air can be used as the cooling medium of the ceramic membrane condenser to recover the water and waste heat from the flue gas, and the effective utilization of the flue gas waste heat can be realized.

#### ■ AUTHOR INFORMATION

##### Corresponding Author

Guoqing Shen – School of Energy, Power and Mechanical Engineering, North China Electric Power University, Beijing 102206, China; Email: [guoqingshen@ncepu.edu.cn](mailto:guoqingshen@ncepu.edu.cn)

##### Authors

Da Teng – School of Energy, Power and Mechanical Engineering, North China Electric Power University, Beijing 102206, China; [orcid.org/0000-0001-6700-4856](https://orcid.org/0000-0001-6700-4856)

Xinxian Jia – School of Energy, Power and Mechanical Engineering, North China Electric Power University, Beijing 102206, China

Wenkai Yang – School of Energy, Power and Mechanical Engineering, North China Electric Power University, Beijing 102206, China

Liansuo An – School of Energy, Power and Mechanical Engineering, North China Electric Power University, Beijing 102206, China

Heng Zhang – School of Energy, Power and Mechanical Engineering, North China Electric Power University, Beijing 102206, China

Complete contact information is available at:  
<https://pubs.acs.org/10.1021/acsomega.1c05610>

#### Notes

The authors declare no competing financial interest.

#### ■ ACKNOWLEDGMENTS

This work is financially supported by the National Key R&D Program of China (2018YFB0604305-05).

#### ■ REFERENCES

- (1) IEA (International Energy Agency). *World Energy Statistics and Balances: Balances*. 2020, Available Online: <https://www.iea.org/data-and-statistics/data-product/world-energy-balances>.
- (2) ZareNezhad, B.; Aminian, A. A Multi-layer Feed Forward Neural Network Model for Accurate Prediction of Flue Gas Sulfuric Acid Dew Points in Process Industries. *Appl. Therm. Eng.* **2010**, *30*, 692–696.
- (3) Bahadori, A. Estimation of Combustion Flue Gas Acid Dew Point During Heat Recovery and Efficiency Gain. *Appl. Therm. Eng.* **2011**, *31*, 1457–1462.
- (4) Zala, S. H.; Parmar, V. M. Energy Loss Estimation Combustion Chamber and Heat Transfer Zones of a Coal Fired Boiler. *Int. J. Adv. Eng. Res. Dev.* **2016**, *3*, 96–102.
- (5) Min, C.; Yang, X.; He, J.; Wang, K.; Xie, L.; Onwude, D. I.; Zhang, W.; Wu, H. Experimental Investigation on Heat Recovery from Flue Gas Using Falling Film Method. *Therm. Sci. Eng. Prog.* **2021**, *22*, 100839.
- (6) Jin, S. M.; Chen, L. Y.; Zhu, Y. C. Analysis of Energy Utilizing Efficiency in a Two Stage Libr-H<sub>2</sub>O Absorption Refrigerator Driver by Waste Heat of Flue Gas. *J. Eng. Thermophys.* **2010**, *31*, 19–23.
- (7) Cui, Z.; Du, Q.; Gao, J. Development of Integrated Technology for Waste Heat Recovery from Humid Flue Gas of Hot Water Boiler. *Int. J. Energy Res.* **2021**, 19560.
- (8) Wang, C.; He, B.; Sun, S.; Wu, Y.; Yan, N.; Yan, L.; Pei, X. Application of a low pressure economizer for waste heat recovery from the exhaust flue gas in a 600 MW power plant. *Energy* **2012**, *48*, 196–202.
- (9) Zhou, N.; Wang, X.; Chen, Z.; Wang, Z. Experimental Study on Organic Rankine Cycle for Waste Heat Recovery from Low-temperature Flue Gas. *Energy* **2013**, *55*, 216–225.
- (10) Xu, W.; Jin, Y.; Zhu, L.; Li, Z. Performance Analysis of the Technology of High-Temperature Boiler Feed Water to Recovery the Waste Heat of Mid-Low-Temperature Flue Gas. *ACS Omega* **2021**, *6*, 26318–26328.
- (11) Xu, G.; Xu, C.; Yang, Y.; Fang, Y.; Li, Y.; Song, X. A Novel Flue Gas Waste Heat Recovery System for Coal-fired Ultra-Supercritical Power Plants. *Appl. Therm. Eng.* **2014**, *67*, 240–249.
- (12) Li, F.; Lin, D.; Fu, L.; Zhao, X. Research and Application of Flue Gas Waste Heat Recovery in Co-generation based on Absorption Heat-exchange. *Procedia Eng.* **2016**, *146*, 594–603.
- (13) Wei, M.; Yuan, W.; Song, Z.; Fu, L.; Zhang, S. Simulation of a Heat Pump System for Total Heat Recovery from Flue Gas. *Appl. Therm. Eng.* **2015**, *86*, 326–332.
- (14) Bo, Y.; Yi, J.; Lin, F.; Shigang, Z. Experimental and Theoretical Investigation of a Novel Full-Open Absorption Heat Pump Applied to District Heating by Recovering Waste Heat of Flue Gas. *Energy and Building* **2018**, *173*, 45–57.
- (15) Yang, B.; Jiang, Y.; Fu, L.; Zhang, S. Experimental and Theoretical Investigation of a Novel Full-open Absorption Heat

Pump Applied to District Heating by Recovering Waste Heat of Flue Gas. *Energy and Buildings* **2018**, *173*, 45–57.

(16) Jiang, C.; Jia, C.; Liu, P.; Li, Z. Analysis of the effect of the ceramic membrane module Based on Epsilon Software on Water Recovery of Flue Gas from Coal-fired Power Plants. *Comput.-Aided Chem. Eng.* **2020**, *48*, 421–426.

(17) Yang, B.; Shen, G.; Chen, H.; Feng, Y.; Wang, L. Experimental Study of Condensation Heat-transfer and Water-recovery Process in a Micro-Porous Ceramic Membrane Tube Bundle. *Appl. Therm. Eng.* **2019**, *155*, 354–364.

(18) Wang, L.; Wang, Z.; Yang, X.; Ru, K.; Song, J. Simulation of Water Recovery in Membrane Condenser Dehumidification Process. *Appl. Therm. Eng.* **2021**, *193*, 117018.

(19) Brunetti, A.; Santoro, S.; Macedonio, F.; Figoli, A.; Drioli, E.; Barbieri, G. Waste Gaseous Streams from Environmental Issue to Source of Water by Using Membrane Condensers. *Clean - Soil, Air, Water* **2014**, *42*, 1145–1153.

(20) Chen, H.; Zhou, Y.; Sun, J.; Liu, Y.; Zhong, Y.; Du, W. An Experimental Study of Membranes for Capturing Water Vapor from Flue Gas. *J. Energy Inst.* **2018**, *91*, 339–348.

(21) Zhang, F.; Ge, Z.; Shen, Y.; Du, X.; Yang, L. Mass Transfer Performance of Water Recovery from Flue Gas of Lignite Boiler by Composite Membrane. *Int. J. Heat Mass Transfer* **2017**, *115*, 377–386.

(22) Gao, D.; Li, Z.; Zhang, H.; Chen, H.; Cheng, C.; Liang, K. Moisture and Latent Heat Recovery from Flue Gas by Nonporous Organic Membranes. *J. Cleaner Prod.* **2019**, *225*, 1065–1078.

(23) Cheng, C.; Zhang, H.; Chen, H. Experimental Study on Water Recovery from Flue Gas Using Macroporous Ceramic Membrane. *Materials* **2020**, *13*, 804.

(24) Chen, H.; Li, X.; Wei, J.; Feng, Y.; Gao, D. Preparation and Properties of Coal Ash Ceramic Membranes for Water and Heat Recovery from Flue Gas. *J. Chem.* **2019**, *11*, 1–10.

(25) Xiao, L.; Yang, M.; Yuan, W. Z.; Huang, S. M. Microporous Ceramic Membrane Condenser for Water and Heat Recovery from Flue Gas. *Appl. Therm. Eng.* **2021**, *186*, 116512.

(26) Chen, H.; Zhou, Y.; Cao, S.; Li, X.; Su, X.; An, L.; Gao, D. Heat Exchange and Water Recovery Experiments of Flue Gas with Using Nanoporous Ceramic Membranes. *Appl. Therm. Eng.* **2017**, *110*, 686–694.

(27) Zhang, H.; Zhang, J.; Liu, Z.; Li, Z.; Chen, H. Simulation Study of Using Microporous Ceramic Membrane to Recover Waste Heat and Water from Flue Gas. *Sep. Purif. Technol.* **2021**, *275*, 119218.

(28) Li, Z.; Zhang, H.; Chen, H.; Zhang, J.; Cheng, C. Experimental Research on the Heat Transfer and Water Recovery Performance. *Appl. Therm. Eng.* **2019**, *160*, 114060.

(29) Gao, D.; Li, Z.; Zhang, H.; Zhang, J.; Chen, H.; Fu, H. Moisture Recovery from Gas-fired Boiler Exhaust Using Membrane Module Array. *J. Cleaner Prod.* **2019**, *231*, 1110–1121.

(30) Wang, T.; Yue, M.; Qi, H.; Feron, P. H. M.; Zhao, S. Transport Membrane Condenser for Water and Heat Recovery from Gaseous Streams: Performance Evaluation. *Appl. Therm. Eng.* **2015**, *484*, 10–17.

(31) Cao, Y.; Wang, L.; Ji, C.; Xue, Z.; Lu, J.; Qi, H. Pilot-scale Application on Dissipation of Smoke Plume from Flue Gas Using Ceramic Membrane Condensers. *J. Chem. Eng.* **2019**, *70*, 2192–2201.

(32) Bao, A.; Wang, D.; Lin, C. Nanoporous Membrane Tube Condensing Heat Transfer Enhancement Study. *Int. J. Heat Mass Transfer* **2015**, *84*, 456–462.

(33) Wang, D. Advanced Energy and Water Recovery Technology from Low Grade Waste Heat. *Office of Scientific & Technical Information Technical Reports*, 2011, DOI: 10.2172/1031483.

(34) Yue, M.; Zhao, S.; Feron, P. H. M.; Qi, H. Multichannel Tubular Ceramic Membrane for Water and Heat Recovery from Waste Gas Streams. *Ind. Eng. Chem. Res.* **2016**, *55*, 2615–2622.

(35) Soleimanikutanaei, S.; Lin, C. X.; Wang, D. Numerical Modeling and Analysis of Transport Membrane Condensers for Waste Heat and Water Recovery from Flue Gas. *Int. J. Therm. Sci.* **2019**, *136*, 96–106.

(36) Zhang, J.; Li, Z.; Zhang, H.; Chen, H.; Gao, D. Numerical Study on Recovering Moisture and Heat from Flue Gas by Means of a Microporous Ceramic Membrane Module. *Energy* **2020**, *207*, 118230.

(37) Li, Z.; Xue, K.; Zhang, H.; Chen, H.; Gao, D. Numerical Investigation on Condensation Mode of the Transport Membrane Condenser. *Int. J. Heat Mass Transfer* **2020**, *161*, 120305.

(38) Cheng, C.; Fu, H.; Zhang, H.; Chen, H.; Gao, D. Study on the Preparation and Properties of Talcum-Fly Ash based Ceramic Membrane Supports. *Membranes* **2020**, *10*, 207.

(39) Zhang, X.; Zhang, L.; Liu, H.; Pei, L. One Step Fabrication and Analysis of an Asymmetric Cellulose Acetate Membrane for Heat and Moisture Recovery. *J. Membr. Sci.* **2011**, *366*, 158–165.

(40) Yang, B.; Chen, H. Heat and Water Recovery from Flue Gas: Application of Micro-Porous Ceramic Membrane Tube Bundles in Gas-fired Power Plant. *Chem. Eng. Process.* **2019**, *137*, 116–127.

(41) Zhao, S.; Wordhaugh, L.; Zhang, J.; Feron, P. H. M. Condensation, Re-evaporation and Associated Heat Transfer in Membrane Evaporation and Sweeping Gas Membrane Distillation. *J. Membr. Sci.* **2015**, *475*, 445–454.

(42) Cheng, C.; Zhang, H.; Chen, H. Experimental Study on Water Recovery and SO<sub>2</sub> Permeability of Ceramic Membranes with Different Pore Size. *Int. J. Energy Res.* **2020**, *44*, 6313–6324.

(43) Teng, D.; An, L.; Shen, G.; Zhang, S.; Zhang, H. Experimental Study on a Ceramic Membrane Condenser with Air Medium for Water and Waste Heat Recovery from Flue Gas. *Membranes* **2021**, *11*, 701.

(44) Kim, J. F.; Park, A.; Kim, S. J.; Lee, P. S.; Cho, Y.; Park, H.; Nam, S. F.; Park, Y. Harnessing Clean Water from Power Plant Emissions Using Membrane Condenser Technology. *ACS Sustainable Chem. Eng.* **2018**, *6*, 6425–6433.